

Utilization of Additive Manufacturing in Evaluating the Performance of Internally Defected Materials

A-H I Mourad^{1*}, A M Ghazal², M M Syam² and O D Al Qadi² and H Al Jassmi³

1 Professor, Department of Mechanical Engineering, UAE University, PO. Box 15551 Al-Ain, UAE

2 Research Scholar, Department of Mechanical Engineering, UAE University, PO. Box 15551 Al-Ain, UAE

3 Assistant Professor, Department of Civil & Environmental Engineering, UAE University, PO. Box 15551 Al-Ain, UAE

* Corresponding author e-mail: ahmourad@uaeu.ac.ae

Abstract. The elimination of internal defects in a material present in the raw material or generated during the manufacturing or service is difficult. The inclusions of the defects have an adverse effect on the load bearing capacity. The presence of the cracks subjected to a specific orientation in materials or machinery can cause devastating unexpected failure during operation. Analysis of the failure in the components with cracks is more confined to analytical and numerical evaluation. The experimental evaluation has been tedious due to the complexity of replicating the actual defected component. The potential of additive manufacturing in developing user-defined components with cracks for the experimental evaluation is explored in this research. The present research investigated the effect of the internal elliptical cracks aligned at different orientations on the mechanical performance of polylactic acid (Green filament). The Fusion Deposition Method was utilized for the development of the standard tensile specimens with internal elliptical crack oriented at 0°, 45° and 90° using UltiMaker 2. The results proved that there is a considerable reduction in the load bearing capacity due to the presence of the cracks. The maximum load bearing capacity decreased by 15.01% for the specimen with crack inclined at 0° to the lateral axis compared to crack-free specimen. The nature of the fracture and the stress-strain graph evidently showcase the brittle nature of the material. The SEM image of the fractured region proved the phenomenal characteristics such as strong adhesion between the layers and the proper material flow. In the light of the results of this work, it can be concluded that the 3-D printing methodology is effective for evaluating the mechanical performance of the internally defected material.

Keywords: Additive Manufacturing (AM); Fused deposition method (FDM); Infill rate; Internal elliptical crack; Mechanical performance.

1. Introduction

There is a crucial need for examining the mechanical properties of structures with internal defects especially in applications where such tiny defects can cause catastrophic failure (i.e., Aerospace or biomedical applications). The above-mentioned problem was solved analytically in the absence of conventional fabrication methods to produce samples with internal defects for experimental testing. For more than a decade, additive manufacturing (AM) or 3D printing has taken the attention due to its beneficial ability to handle a high level of complexity in terms of geometry and material, which could



not be fabricated by subtractive manufacturing methods in rapid prototyping (RP). This technology is defined as a process for producing three-dimensional (3D) objects from Computer-Aided Design (CAD models) through an additive process in which successive layers adds sequentially [1]. Fused deposition modelling (FDM), selective laser melting (SLM) and selective laser sintering (SLS) are commonly used techniques to take advantage of material extrusion. Additional to variant methods of 3D printing technologies in the early 1990s, the Laminated Object Manufacturing (LOM) has developed by Helisys of Torrance which provides a laminated concept in 3D printing [2].

Among AM technologies, the fused deposition modelling (FDM) has the largest share from the most widely used techniques. This technique has been firstly developed by Stratasys Inc. since last century. According to the 2011 Wohler's Report, the FDM currently has reached 41.5 percent of the used 3D systems commercially [3]. The technique used the advantage of thermoplastic materials by continuous extrusion and deposition with solidification properties of the material [4]. FDM has three key elements in the system including material feed mechanism, liquefier/print head and building surface.

Figure 1 shows the main components of FDM 3D printer [5, 6]. Two materials are commonly processed by such technology namely acrylonitrile butadiene styrene (ABS) and polylactic acid (PLA) as FDM filaments, which will be extruded through the liquefier to the printing nozzle which is illustrated in flow diagram depicted in figure 2 [7]. PLA is proven to be a stronger alternative than ABS for FDM technologies as reported in the literature. H. Kim et al. [7] reported that PLA has higher tensile strength as compared to ABS. It was noted that the liquefied PLA thread has a stronger bonding than the liquefied ABS thread, which was observed from the failure surface.

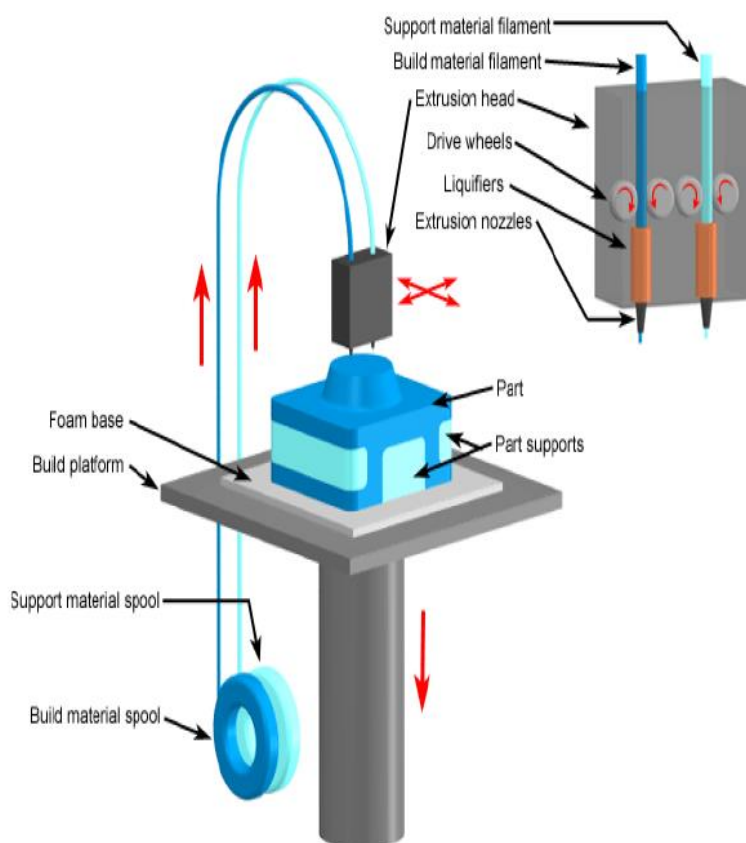


Figure 1. Fused deposition modeling 3D printer [6]

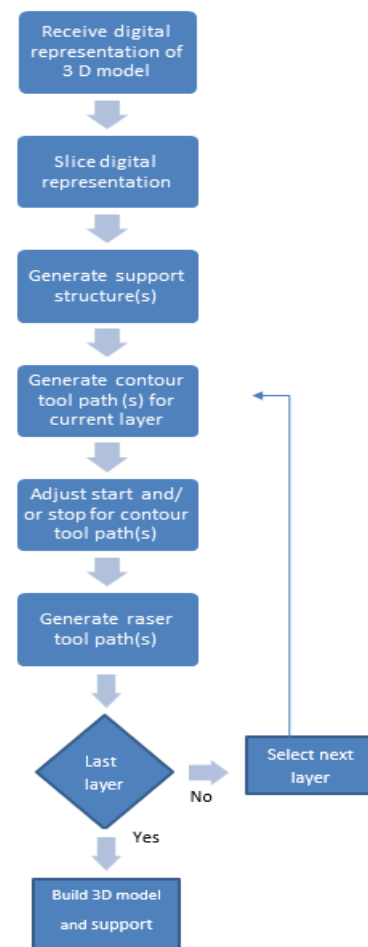


Figure 2. FDM procedure diagram

Polylactic acid (PLA) is a biodegradable thermoplastic derived from sugar and starch. It has malleable behaviour when it is heated, which allows for various shapes' creation. As far as the mechanical properties are concerned, PLA is a brittle material that has relatively high tensile and flexural moduli and has good stiffness and strength [8]. Letcher and M. Waytashek [9] have tested 3D printed PLA material of different raster angles (0° , 45° and 90°) under tension, flexural and fatigue loadings to evaluate the material's properties. Tensile tests revealed that the 45° raster angle resulted in the strongest fabricated samples. However, the flexural testing showed that the raster angle of 0° resulted in the highest bending stress among the tested samples. As far as the fatigue testing results are concerned, both 0° and 45° raster angles resulted in almost similar behaviour that was better than the one attained at 90° . In addition, B. Witt Brodt and J. Pearce [10] have investigated the effect of the PLA colour (i.e., natural, white, blue, grey and black) on the mechanical properties of the material. Conducted tensile testing (refer to table 1) showed that the highest strength occurred for natural colour, whereas the lowest one was attained by the grey colour. It should be noted that the authors had assessed the effect of extrusion temperature (i.e., 190°C to 215°C) on the tensile strength and crystallinity percentage for the white colour. The results had revealed that the increase in extrusion temperature results in increasing the tensile strength in general; however, the 200°C tests showed out-of-trend behaviour, which was justified by the preference direction of the developed grains. Also, there was an existence for a maximum extrusion temperature at which the maximum crystallinity percentage occurs.

Table 1. Properties of PLA [10].

Colour	Ultimate tensile strength (MPa)	Yield strength (MPa)	Maximum strain (%)	Crystallinity (%)
Natural	57.16 ± 0.35	52.47 ± 0.35	2.35 ± 0.05	0.93 ± 0.06
Black	52.81 ± 1.18	49.23 ± 1.18	2.02 ± 0.08	2.62 ± 0.09
Grey	50.84 ± 0.23	46.08 ± 0.23	1.98 ± 0.04	4.79 ± 0.10
Blue	54.11 ± 0.30	50.10 ± 0.30	2.13 ± 0.02	4.85 ± 0.15
White	53.97 ± 0.26	50.51 ± 0.26	2.22 ± 0.04	5.05 ± 0.18

J. Chacón et al. [11] have investigated the effect of 3D printing process parameters on the mechanical properties of printed PLA structures. In this study, building orientation, layer thickness and feed rate were varied and their consequence effect on the tensile and three-point bending was examined. D. Farbman and C. McCoy [12] have studied the effect of infill percentage (0% up to 100%), infill orientation (rectilinear and hexagonal) and strain rate (up to 15 mm/second) on the mechanical performance of ABS and PLA material. It was concluded that the higher infill percentages result in stronger samples.

The main objectives of the research are to produce 3D printed standard tensile samples with and without internal elliptical defects and to examine the effect of elliptical internal defects on the mechanical performance of the 3D printed PLA structures considering different orientations (0° , 45° and 90°). The capability of utilizing additive manufacturing for evaluating the mechanical performance of defected materials could be a major advantage in near future. The production of defect-free specimens with high quality are mandatory for adopting the technique. The effect of the parameters on the quality is dominant and the current study evaluates the afore-mentioned aspects.

2. Materials and Methods

In the present work, a commercial type of green PLA filament with 2.85mm diameter was opted for the experimentations. The mechanical properties of the PLA manufactured by FDM is shown in table 2.

Table 2. Mechanical properties of PLA [13, 14].

Properties	Value
Tensile strength (MPa)	15.5-72.2
Tensile modulus (GPa)	2.020-3.550
Elongation at break (%)	0.5-9.2

ASTM D638 standard for the polymers testing was followed due to lack of an international standard for the evaluation of the mechanical properties of 3D printed specimens. The tensile specimen model with internal elliptical cracks was modelled in CATIA V5 and exported to .stl format. Figure 3 shows the geometrical dimensions of the standard tensile specimen.

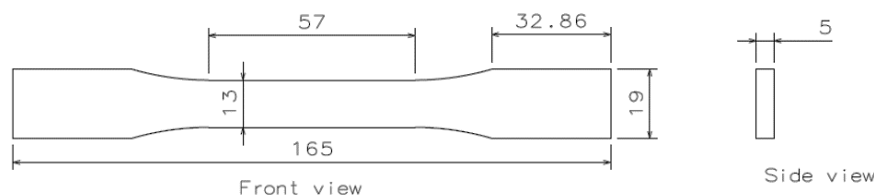
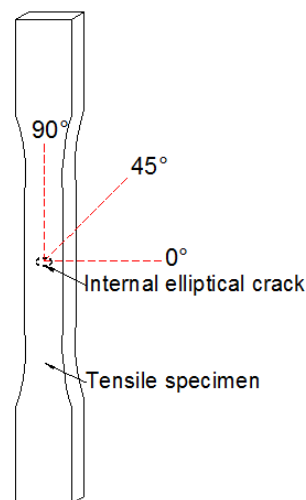
**Figure 3.** Geometrical dimension of the tensile specimen. All dimensions in mm.

Figure 4 presents a 3D schematic drawing showing the crack orientations. The crack length ($2c$) and crack width ($2a$) are 2mm and 1mm, respectively, for the internal elliptical crack.

**Figure 4.** 3D Schematic drawing of the tensile specimen showing different crack orientations.

Different specimens with crack orientations of 0° , 45° and 90° to the lateral axis are fabricated. The results are compared with the crack-free specimens.

2.1 Process Parameters

PLA colour type, raster angle, printing layer thickness, feed rate and infill rate are the major process parameters used for FDM 3D printing process. These used process parameters are given in table 3.

Table 3. Process parameter for FDM technique.

PARAMETERS	VALUE / SPECIFICATION
PLA (colours)	Green
Layer thickness (mm)	0.1
Shell wall thickness (mm)	1.05
Shell top/bottom thickness (mm)	0.8
Infill percentage (%)	100 %
Feed rate/printing speed (mm/s)	80
Raster angle	45 °
Extruding temperature	228 °C

2.2 Tensile Testing

The PLA specimens were tested using E45.305 tensile testing machine produced by MTS and equipped with 100 KN load cell. The tests were conducted at 0.25 mm/s. Total of eighteen tensile samples was tested under standard room temperature (25°C) since the thermoplastic material is very dependent on the temperature. In addition, MTS axial extensometer (MODEL 632,25F-20) has been used for strain measurements.

2.3 Scanning Electron Microscopy (SEM)

Scanning Electron Microscopy (SEM) images were taken at the fractured surfaces after the tensile testing. The SEM - JSM-6010LA developed by JEOL was used in this study. Generally, the SEM images are capable of providing high resolution with fine detailed images to identify and quantify the compositional information and surface topography. The machine used in this study can provide a resolution of 4 nm and a magnification power ranging from 5X up to 300,000X. The device can handle a specimen size up to 150 mm diameter [15].

3. Results and Discussions

The presence of the internal cracks is expected to lower down the load bearing capacity of the material. In the presence of the crack, it is more vital to evaluate the maximum load bearing capacity of the material before fracture than the tensile strength of the specimen. The tensile strength is analytically calculated as the ratio of peak tensile force to the cross-sectional area. The load-displacement curve and stress-strain graph for the crack-free specimen are shown in figure 5. The lack of sufficient yielding before fracture in the stress-strain graph proves the brittleness of the PLA-green specimen. The modulus of elasticity for the non-defected PLA-green sample calculated from the stress-strain graph is 2774 MPa. This value is within the ranges reported in the table 2 (2020 MPa – 3550 Mpa).

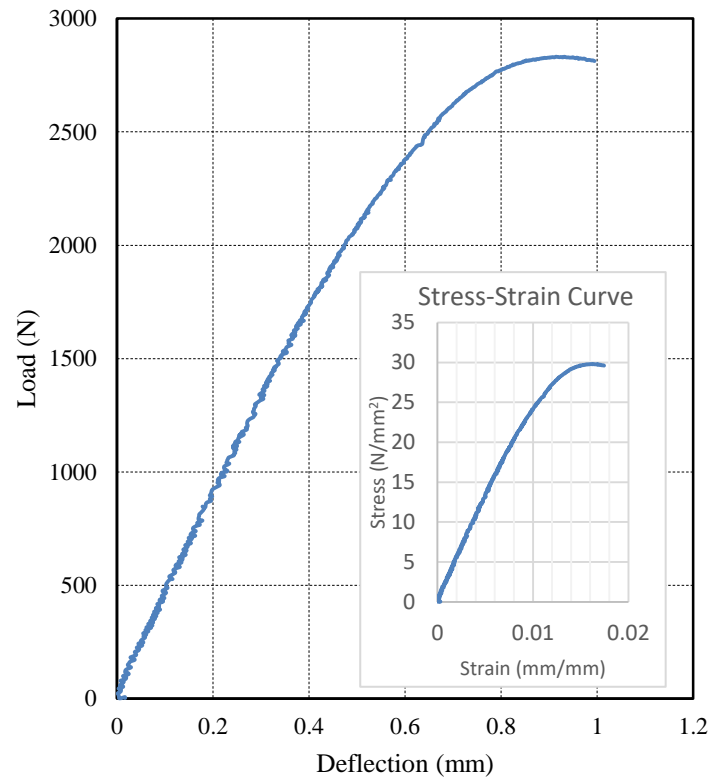


Figure 5. Load-deflection curve and stress-strain graph for crack-free PLA specimen (Green)

The presence of the cracks lessens the cross-sectional area of the sample. The determination of the tensile strength is inappropriate in such circumstances. In such situation, two approaches can be used to evaluate the load bearing capacity of the specimen. These are the fracture mechanics approach in which the stress intensity factor is the characterizing parameter or the stress concentration approach. Figure 6 shows the load-displacement curves obtained for the PLA-green specimens with crack oriented at 0°, 45° and 90° and without a crack. The graphs clearly indicated the brittle nature of the specimen. The specimens with crack and without crack resulted in the same trend. Three separate regions may be classified based on the load displacement distributions. The stiffness (Young's modulus) is constant in the first region in which the Hooke's law is applicable whereas the stiffness decreases slightly in the second region. There is more reduction in the stiffness in the third region before the fracture. The load-displacement curves indicate that the crack free specimen possess more load withstand ability. The cracks found to depreciate the load carrying capacity of the material. The result signifies the relevance of avoiding the cracks from the materials that are subjected to load conditions. The orientation has found to have profound relevance in terms of the load bearing capacity.

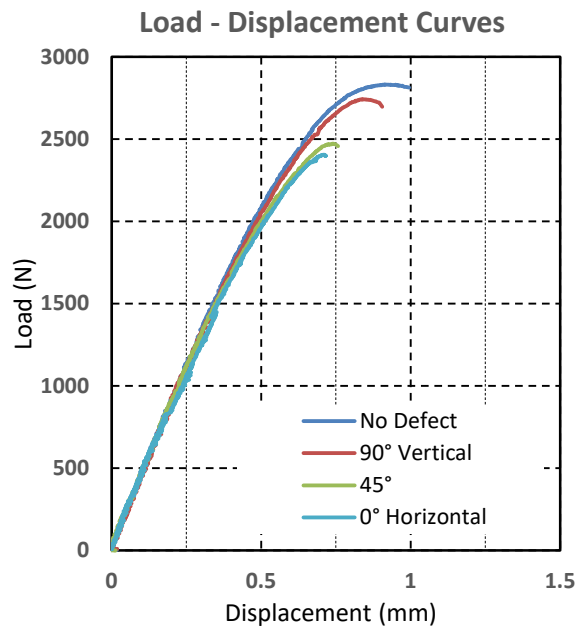


Figure 6. Force - Displacement of the PLA (green)

The load bearing capacity of the sample with crack oriented 90° to the lateral axis is more than the specimen having the crack oriented 0° to the lateral axis. The load bearing capacity of the PLA-green specimen with crack inclined 45° to the lateral axis is nearly close to that of the specimen with crack oriented at 0° .

The bar chart shown in figure 7 shows the maximum load carrying capacity of the crack and crack-free specimens. The maximum withstanding load before the fracture for the defect free specimen was 2830 N whereas the peak loads were 2743 N, 2472 N and 2405 N for the specimens with crack inclined at 90° , 45° and 0° respectively. The peak load decreased as the angle of orientation to the lateral axis is decreased. A reduction of 15.01% in the peak load, compared to the defect-free sample, is recorded for the sample of 0° orientation. These peak load values are considerably reduced compared to cracked specimen oriented 90° to the lateral axis. The closeness of the peak load for the defect-free and 90° crack-oriented specimen is also observed. The load-displacement graph reveals that the defect size was found to have no influence on the slope of the load-displacement graph (i.e., stiffness of the material).

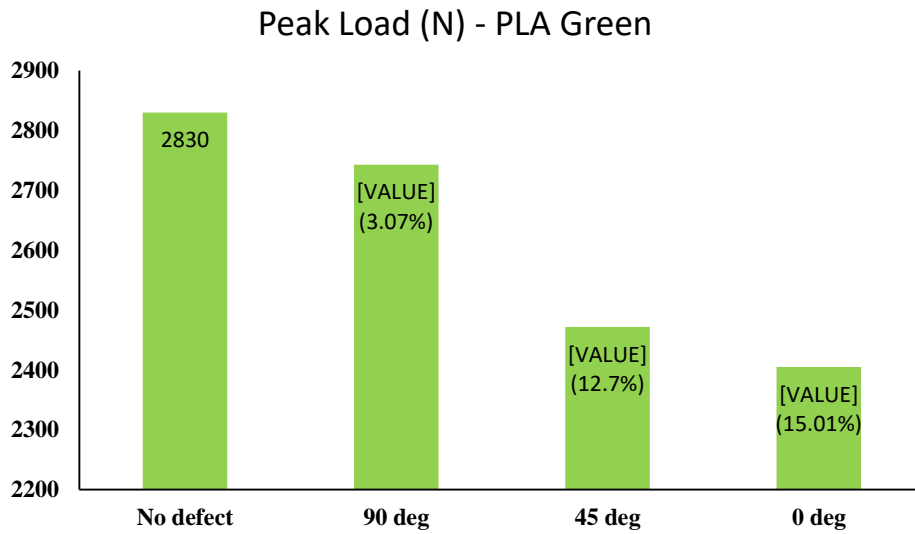


Figure 7. Effect of the defect’s orientation on the peak load

The reduction of the peak load when the crack inclines towards the lateral axis causes an increase in the normal opening stress which is the weak link of brittle material. The internal defected samples were fractured exactly at the center of the gauge length where the crack was present as shown in figure 8. It is observed that the mode of fracture is brittle and there is no evidence for any necking which support the observation from the load-displacement curves.

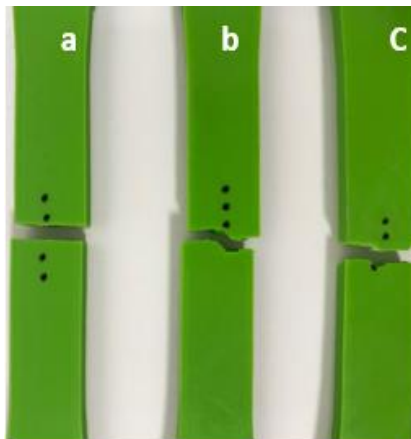


Figure 8. Fractured samples of samples oriented at (a) 0 °, (b) 45 °, and (c) 90 °

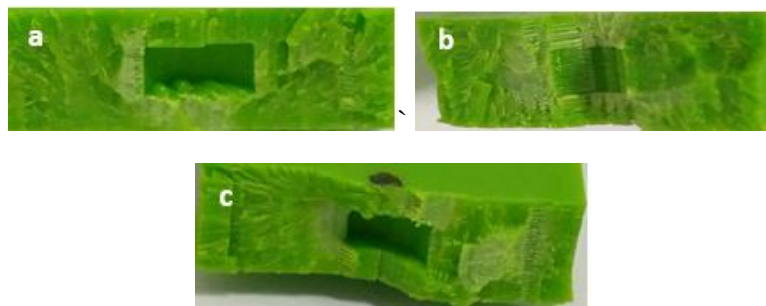


Figure 9. Fracture surfaces (a) 0 °, (b) 90 °, and (c) 45 °

Figure 9 shows the fractured surfaces of the specimen with cracks oriented at different angles. The fracture surface topography shows that the material is porous-free with smooth appearance. This is the main reason of getting the expected trend and the high level of repeatability of the results. Such evidence prove that the 3D printing technique can be used to produce quality samples that can be employed for studying and evaluating the mechanical properties of defected and defect-free materials. The enlarged optical image and the SEM image of the fractured surface are shown in figure 10 and figure 11 respectively. Figure 10 shows that the fracture surface is smooth and porous-free to a large extent. This reflects the proper flow of the molten material.



Figure 10. Magnified Optical Images (10x) at the fractured surface – PLA Green

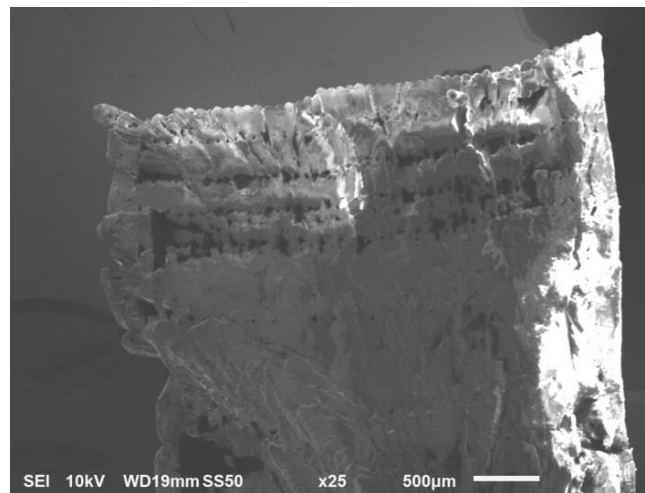


Figure 11. SEM Image of the fractured surface - PLA Green (25x)

The melting and solidification of the material that has been laid by layers is the fundamental characteristic of additive manufacturing. The SEM image of the fracture surface in figure 11 shows strong adhesion between the layers and the proper flow of the material. This could result in the absence of the layering and the pores that may be suspected even at 100% infill rate. Presence of the voids or gaps anticipated at lower infill rate could deteriorate the mechanical performance. There is a smooth build-up of the material far from the edges or shell material. The smoother builds up imply stronger inter-layer fusion bonds between the different layers; hence, expected to have higher stress values [16]. No layer separation showcases the unique property of the 3D printing to develop materials layer by layer forming a defect-free solid rigid object that can be used to assess the mechanical characterization of the material with and without defects. The results shows also that the additive manufacturing/3D

printing method can be utilized to characterize the stable crack growth through materials [17-21] with minimum number of samples.

4. Conclusion

The research focused on examining the effect of internal elliptical crack on the mechanical performance of 3D-Printed PLA (Green filament). Crack and crack-free specimens fabricated according to ASTM D638 were printed using UltiMaker 2. The specimens with elliptical crack inclined 0°, 30° and 90° to the lateral axis are investigated. The crack-free specimen has the maximum load capacity. The load bearing capacity reduced considerably due to the presence of internal elliptical cracks. The reduction of the maximum load for the specimen with cracks oriented at 0°, 45° and 90° to the lateral axis compared to crack-free PLA (green filament) specimen accounted to 15.07%, 12.7% and 3.07% respectively. The defected samples fractured exactly at the center of the gauge length where the crack was present. The SEM images of the fractured surfaces are captured. No layering in the SEM image of the fractured surface showcase strong adhesion among the layers. The smooth buildup of the material from the edges or shell is noticed. The results of this work proved that the additive manufacturing is a promising technique for creating well specified internal cracks in a specimen or component. Therefore, it can be utilized in accurately evaluating the mechanical performance of materials. The number of experiment runs can be reduced for the repeatability tests. This will reflect on the cost of the test. Less number of experiment runs, low cost, less time and easiness to fabricate a predefined crack are the major advantages of utilizing 3D printing. Applicability of additive manufacturing involves the characterization of the internal defect and to predict the performance of internal defected specimens. The future scope of the research is to inspect different parameters such as PLA pigment, infill rate, printing speed on the mechanical performance of the material. The metallic materials with internal defects need to be investigated.

5. References

- [1] Lee, Dongkeon, Takashi Miyoshi, Yasuhiro Takaya, and Taeho Ha. "3D microfabrication of photosensitive resin reinforced with ceramic nanoparticles using LCD microstereolithography." *J. Laser Micro/Nanoeng.* 1 (2006): 142-148.
- [2] Parandoush, Pedram, and Dong Lin. "A review on additive manufacturing of polymer-fiber composites." *Composite Structures* 182 (2017): 36-53.
- [3] Caffrey, T. "Additive manufacturing and 3D printing state of the industry annual worldwide progress report." *Engineering Management Research* 2, no. 1 (2013): 209-222.
- [4] Kruth, J-P., Ming-Chuan Leu, and Terunaga Nakagawa. "Progress in additive manufacturing and rapid prototyping." *Cirp Annals* 47, no. 2 (1998): 525-540.
- [5] V. G. Gokhare, D. N. Raut, D. K. Shinde "A Review paper on 3D-Printing Aspects and Various Processes Used in the 3D-Printing" *International Journal of Engineering Research & Technology (IJERT)* 6 (2017): 953-958
- [6] N. Turner, Brian, Robert Strong, and Scott A. Gold. "A review of melt extrusion additive manufacturing processes: I. Process design and modeling." *Rapid Prototyping Journal* 20, no. 3 (2014): 192-204.
- [7] Kim, Heechang, Eunju Park, Suhyun Kim, Bumsoo Park, Namhun Kim, and Seungchul Lee. "Experimental Study on Mechanical Properties of Single-and Dual-material 3D Printed Products." *Procedia Manufacturing* 10 (2017): 887-897.
- [8] Auras, Rafael A., S. Paul Singh, and Jagjit J. Singh. "Evaluation of oriented poly (lactide) polymers vs. existing PET and oriented PS for fresh food service containers." *Packaging technology and science* 18, no. 4 (2005): 207-216.
- [9] Letcher, Todd, and Megan Waytashek. "Material property testing of 3d-printed specimen in PLA on an entry-level 3d printer." In *ASME 2014 International Mechanical Engineering Congress and Exposition*, pp. V02AT02A014-V02AT02A014. American Society of Mechanical Engineers, 2014.

- [10] Wittbrodt, Ben, and Joshua M. Pearce. "The effects of PLA color on material properties of 3-D printed components." *Additive Manufacturing* 8 (2015): 110-116.
- [11] Chacón, J. M., M. A. Caminero, E. García-Plaza, and P. J. Núñez. "Additive manufacturing of PLA structures using fused deposition modelling: effect of process parameters on mechanical properties and their optimal selection." *Materials & Design* 124 (2017): 143-157.
- [12] Farbman, Daniel, and Chris McCoy. "Materials Testing of 3D Printed ABS and PLA Samples to Guide Mechanical Design." In *ASME 2016 11th International Manufacturing Science and Engineering Conference*, pp. V002T01A015-V002T01A015. American Society of Mechanical Engineers, 2016.
- [13] Kotlinski, Jaroslaw. "Mechanical properties of commercial rapid prototyping materials." *Rapid Prototyping Journal* 20, no. 6 (2014): 499-510.
- [14] Lanzotti, Antonio, Marzio Grasso, Gabriele Staiano, and Massimo Martorelli. "The impact of process parameters on mechanical properties of parts fabricated in PLA with an open-source 3-D printer." *Rapid Prototyping Journal* 21, no. 5 (2015): 604-617.
- [15] JSM – 6510 SERIES user manuals, 1st ed, JEOL Ltd, 2014.
- [16] Torrado, Angel R., and David A. Roberson. "Failure analysis and anisotropy evaluation of 3D-printed tensile test specimens of different geometries and print raster patterns." *Journal of Failure Analysis and Prevention* 16, no. 1 (2016): 154-164.
- [17] Maiti, S. K., G. Krishna Kishore, and Mourad, A.-H. I. "Bilinear CTOD/CTOA scheme for characterisation of large range mode I and mixed mode stable crack growth through AISI 4340 steel." *Nuclear Engineering and Design* 238, no. 12 (2008): 3175-3185.
- [18] Maiti, S. K., S. Namdeo, and Mourad, A.-H. I. "A scheme for finite element analysis of mode I and mixed mode stable crack growth and a case study with AISI 4340 steel." *Nuclear Engineering and Design* 238, no. 4 (2008): 787-800.
- [19] Mourad, A.-H. I., M. J. Alghafri, OA Abu Zeid, and S. K. Maiti. "Experimental investigation on ductile stable crack growth emanating from wire-cut notch in AISI 4340 steel." *Nuclear engineering and design* 235, no. 6 (2005): 637-647.
- [20] Ahmed, W. K., and Mourad, A.-H. I. "Fracture assessment of strengthened cracked metallic components using FRP stiffeners." *Mechanics of Composite Materials* 51, no. 3 (2015): 301-312.
- [21] Mourad, Abdel-Hamid I. "Pure shear stable crack growth through Compact-Tension-Shear specimen in plane state of stress." *Strength, fracture and complexity* 2, no. 3 (2004): 111-125.